Efficient High-Frequency Spin-Torque Oscillators Composed of Two Three-Layer MgO-MTJs with a Common Free Layer

Alexander Makarov, Thomas Windbacher, Viktor Sverdlov, and Siegfried Selberherr
Institute for Microelectronics, TU Wien, Gußhausstraße 27-29/E360, A-1040 Wien, Austria
E-mail: {makarov|windbacher|sverdlov|selberherr}@iue.tuwien.ac.at

***Abstract*—We present a novel spin-torque oscillator based on two three-layer MgO-MTJs with a shared free layer. By performing extensive micromagnetic simulations we found that the structure exhibits a wide tunability of oscillation frequencies from a few GHz to several tens of GHz. We discuss the optimization of such structures in order to obtain the maximum output power.**

Keywords—spin-torque; oscillator; micromagnetic simulation; MgO-MTJ

I. INTRODUCTION

New types of spintronic devices utilizing all-electrical magnetization manipulation by current, such as spin-torque transfer random access memory (RAM) and spin-torque oscillators, have been intensely developed based on MgO magnetic tunnel junctions (MTJs) with a large magneto-resistance ratio [1]. Depending on the orientation of the MTJ magnetization, the devices can be classified in two categories: "perpendicular" with an out-of-plane magnetization direction and "in-plane" with the magnetization lying in the plane of the magnetic layer. Spin-torque oscillators based on MTJs with in-plane magnetization [2] show high frequency capabilities, but still need an external magnetic field and/or are characterized by low output power [3]. Oscillators based on MTJs with perpendicular magnetization [4] and vortex-based oscillators [5] are known to generate oscillations without an external magnetic field; however, their low operating frequencies, usually below 2GHz, limit their functionality and applicability as a tunable oscillator [3].

In [6] a bias-field-free spin-torque oscillator based on an in-plane MgO-MTJ with an elliptical cross-section and without perfect overlap between the free layer and the fixed magnetic layers was proposed. A disadvantage of this architecture is a narrow range of applicable frequencies and their weak dependence on the current density.

In [7] a novel design for spin-torque oscillators composed of two penta-layer in-plane MgO-MTJs with a shared free layer was proposed (Fig.1a). As has been shown in [7], this structure demonstrates stable oscillations with a constant amplitude (Fig.2), high applicable frequency (Fig.3), and operation without a biasing field.

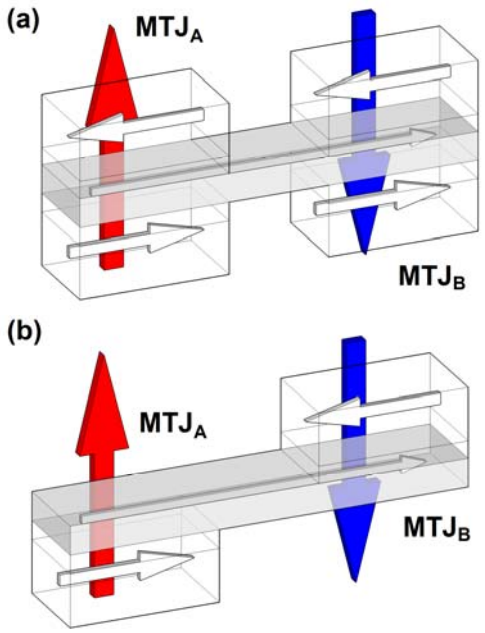

Figure 1. Schematic illustration of a spin-torque oscillator based on: (a) two penta-layer MgO-MTJs and (b) two three-layer MgO-MTJs. Colored arrows indicate the positive direction of the current for each of the MgO-MTJs. The interaction between different areas occurs due to the magnetic exchange interaction and magnetostatic coupling.

In this work we study spin-torque nano-oscillators composed of two three-layer in-plane MgO-MTJs with a shared free layer (Fig.1b). We additionally discuss the optimization of such structures in order to obtain the maximum output power.

This research is supported by the European Research Council through the grant #247056 MOSILSPIN.

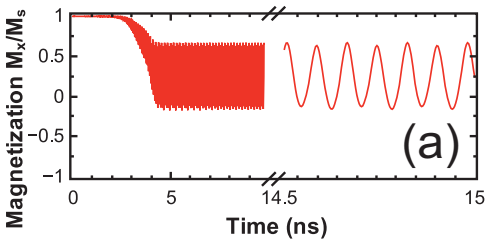

Figure 2. Magnetization components in MTJ_B as a function of time for a free layer of 50×10nm^2: (a) x-component; (b) y-component; (c) z-component. The current densities through MTJ_A and MTJ_B are $7.5\cdot10^7$ A/cm^2 and $1\cdot10^7$ A/cm^2, respectively.

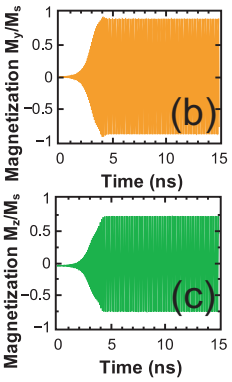

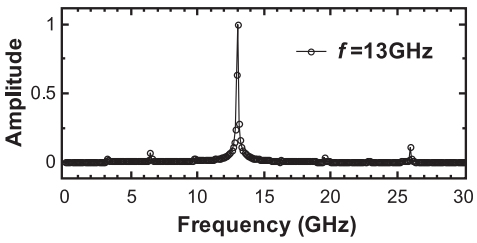

Figure 3. Signal spectral density normalized to its maximum value. The current densities through MTJ_A and MTJ_B are $7.5\cdot10^7$ A/cm^2 and $1\cdot10^7$ A/cm^2, respectively. The peak of the amplitude is observed at a frequency of 13GHz.

II. Model Description

Our simulations of MTJs are based on the magnetization dynamics described by the Landau-Lifschitz-Gilbert-Slonczewski (LLGS) equation in the areas of current flow [8]:

$$\frac{d\mathbf{m}}{dt} = -\frac{\gamma}{1+\alpha^2}\cdot\left((\mathbf{m}\times\mathbf{h}_{\mathbf{eff}})+\alpha\cdot\left[\mathbf{m}\times(\mathbf{m}\times\mathbf{h}_{\mathbf{eff}})\right]\right) + \frac{g\mu_B j}{e\gamma M_s d}\cdot\left(g(\theta_1)\cdot(\alpha\cdot(\mathbf{m}\times\mathbf{p}_1)-[\mathbf{m}\times(\mathbf{m}\times\mathbf{p}_1)]) - g(\theta_2)\cdot(\alpha\cdot(\mathbf{m}\times\mathbf{p}_2)-[\mathbf{m}\times(\mathbf{m}\times\mathbf{p}_2)])\right) \quad (1)$$

and the Landau-Lifschitz-Gilbert (LLG) equation otherwise:

$$\frac{d\mathbf{m}}{dt} = -\frac{\gamma}{1+\alpha^2}\cdot\left((\mathbf{m}\times\mathbf{h}_{\mathbf{eff}})+\alpha\cdot\left[\mathbf{m}\times(\mathbf{m}\times\mathbf{h}_{\mathbf{eff}})\right]\right). \quad (2)$$

Here, γ=2.3245·10^{5}m/(A·s) is the gyromagnetic ratio, α is the Gilbert damping parameter, μ_B is Bohr's magneton, j is the current density, e is the electron charge, d is the thickness of the free layer, $\mathbf{m}=\mathbf{M}/M_s$ is the position dependent normalized vector of the magnetization in the free layer, and $\mathbf{p}_1=\mathbf{M}_{p1}/M_{sp1}$ and $\mathbf{p}_2=\mathbf{M}_{p2}/M_{sp2}$ are the normalized magnetizations in the first and second pinned layers, respectively. M_s, M_{sp1}, and M_{sp2} are the saturation magnetizations of the free layer, the first pinned layer, and the second pinned layer, respectively.

For the function $g(\theta)$ we use Slonczewski's expression for the MTJ with a dielectric layer [9]:

$$g(\theta) = 0.5\cdot\eta\cdot\left[1+\eta^2\cdot\cos(\theta)\right]^{-1}, \quad (3)$$

where η is the spin polarization factor and θ is the angle between the magnetization direction of the free layer and the pinned layer.

The local effective magnetic field is calculated as [10]:

$$\mathbf{h}_{\mathbf{eff}} = \mathbf{h}_{\mathbf{ext}} + \mathbf{h}_{\mathbf{ani}} + \mathbf{h}_{\mathbf{exch}} + \mathbf{h}_{\mathbf{demag}} + \mathbf{h}_{\mathbf{th}} + \mathbf{h}_{\mathbf{amp}} + \mathbf{h}_{\mathbf{ms}}, \quad (4)$$

where $\mathbf{h}_{\mathbf{ext}}$ is the external field, $\mathbf{h}_{\mathbf{ani}}$ is the magnetic anisotropy field, $\mathbf{h}_{\mathbf{exch}}$ is the exchange field, $\mathbf{h}_{\mathbf{demag}}$ is the demagnetizing field, $\mathbf{h}_{\mathbf{th}}$ is the thermal field, $\mathbf{h}_{\mathbf{amp}}$ is the Ampere field, and $\mathbf{h}_{\mathbf{ms}}$ is the magnetostatic coupling between the pinned layers and the free layer.

III. Results And Discussion

Simulations have been performed for a nanopillar CoFeB(5nm)/MgO(1nm)/CoFeB(1.25nm) MTJ, with fixed layers 20×10nm^2 and different free layer lengths ranging from 40nm to 60nm. The other model parameters are: T=300K, $M_s=M_{sp}$=8.9·10^{5}A/m, A=1·10^{-11}J/m, K=2·10^3 J/m^3, α=0.005, and η=0.63 [11].

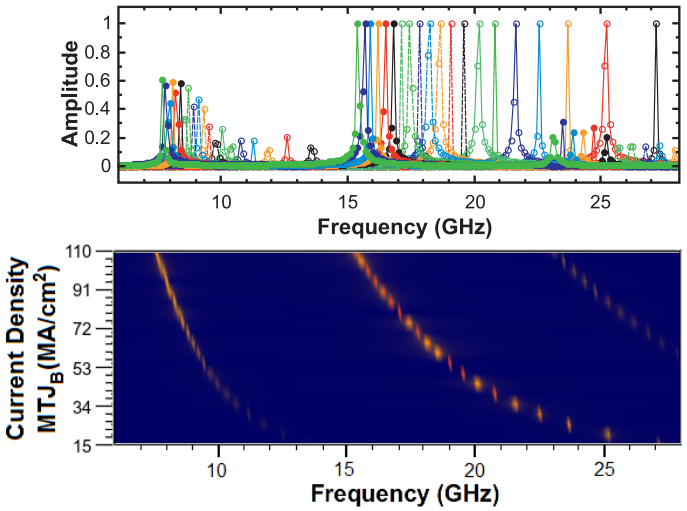

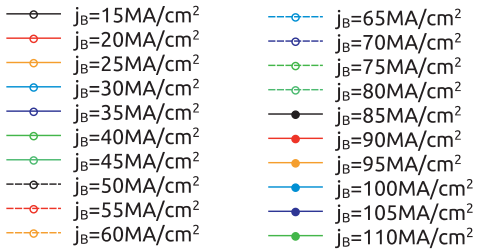

Figure 4. Signal spectral density normalized to its maximum value. The length of the free layer is 40nm. The current density through MTJ_B varies from $1.5\cdot10^7$ to $1.1\cdot10^8$ A/cm^2, while in MTJ_A it is fixed to $2.05\cdot10^8$ A/cm^2.

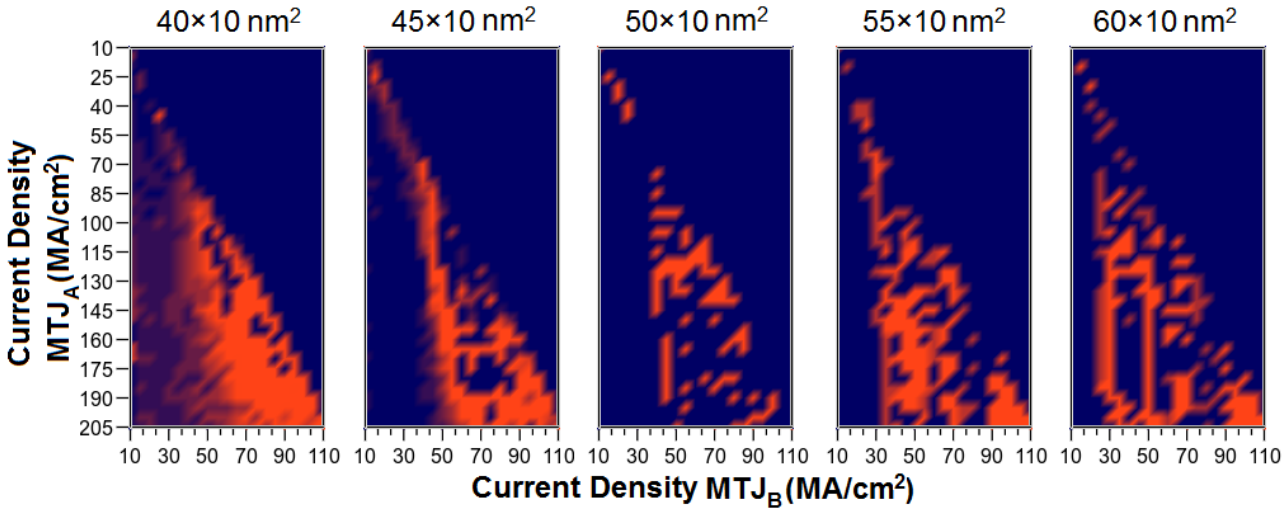

Figure 5. Schematic illustration of the geometrical dependence of the oscillation regime on the current densities through MTJ_A and MTJ_B. The dependencies are shown for five lengths of the free layer: 40nm, 45nm, 50nm, 55nm, and 60nm. The current density through MTJ_A varies from $1 \cdot 10^7$ to $2.05 \cdot 10^8$ A/cm^2 ($j_B \leq j_A/2$). The combinations of current densities at which the amplitude of the additional oscillation mode ($f/2$) reaches a value higher than half the maximum amplitude for the primary oscillation mode (f) are shown in orange color.

First we examine for the presence of an additional oscillation mode with a frequency different from the primary frequency for this structure. We considered a structure with a 40nm free layer length. The current density through MTJ_B varies between $1.5 \cdot 10^7$ and $1.1 \cdot 10^8$ A/cm^2, while in MTJ_A the current density is fixed to $2.05 \cdot 10^8$ A/cm^2. This structure shows stable oscillations for all examined current densities (Fig.4, top). We have found that, apart from the primary oscillation mode at a frequency f, the structure shows an oscillation mode at a frequency of $f/2$ (Fig.4, bottom). The amplitude of this mode increases with increasing current density through MTJ_B and can achieve a higher value than half the maximum amplitude at the primary oscillation mode. The appearance of such an oscillation mode leads to a loss of output power for the main frequency f.

Next we investigated the influence of the free layer geometry and the current densities through the MTJs on the presence of additional oscillation modes. We examined structures with free layer lengths ranging from 40nm to 60nm using 5nm steps. The current density through MTJ_A varies from $1 \cdot 10^7$ to $2.05 \cdot 10^8$ A/cm^2 ($j_B \leq j_A/2$). The step width is $5 \cdot 10^6$ A/cm^2 for both current densities. Our results (Fig.5) indicate that increasing the length of the free layer and thereby the distance between the MgO-MTJs shifts the region, where the additional oscillation mode with a critically large amplitude is observed, towards the region with a larger j_A/j_B ratio. Therefore, the largest variation in the current density at which the additional mode does not reach large amplitudes is observed in the structure with a 40nm free layer length.

Due to the fact that the output power depends on the projection of the oscillations' amplitude $(m_{max}-m_{min})/2$ on the fixed reference layers, amplitude directly reflects the difference between the two extremes in the magnetization oscillations, our next step of optimizing the structure was to determine the dependence of the frequency and magnetization amplitude on the geometry of the free layer and the current densities. Fig.6 shows the dependencies for five lengths of the free layer (40nm, 45nm, 50nm, 55nm, and 60nm) and the current density at which the amplitude of the additional oscillation mode ($f/2$) does not reach a value higher than half the maximum amplitude of the primary oscillation mode (f). Note that the investigated structures show the highest oscillation frequency at ~30GHz (Fig.6a).

In addition to our previous results [7] which show that increasing the ratio j_A/j_B increases the oscillation frequency, we found that increasing the length of the free layer, and as a consequence the increase of the distance between the MTJs leads to a change in the opposite direction, i.e. increasing the ratio j_A/j_B decreases the oscillation frequency. This is more clearly seen in Fig.6e. The magnetization oscillation amplitude depends on the geometry and current density in an inverse manner to that of the frequency.

IV. Conclusion

We investigated a concept of spin-torque oscillators based on two three-layer MgO-MTJs with a shared free layer, which shows stable oscillations without an external magnetic field. The operating frequency of stable oscillations can be tuned for a wide range of frequencies by varying the current densities flowing through the MTJs.

We found the appearance of additional oscillation modes in the investigated structures. An amplitude higher than half the maximum amplitude of the primary oscillation mode can be reached. The presence of such an oscillation mode leads to a loss of output power. The demonstrated ability to exclude additional parasitic oscillation modes makes this structure attractive for potential high power applications.

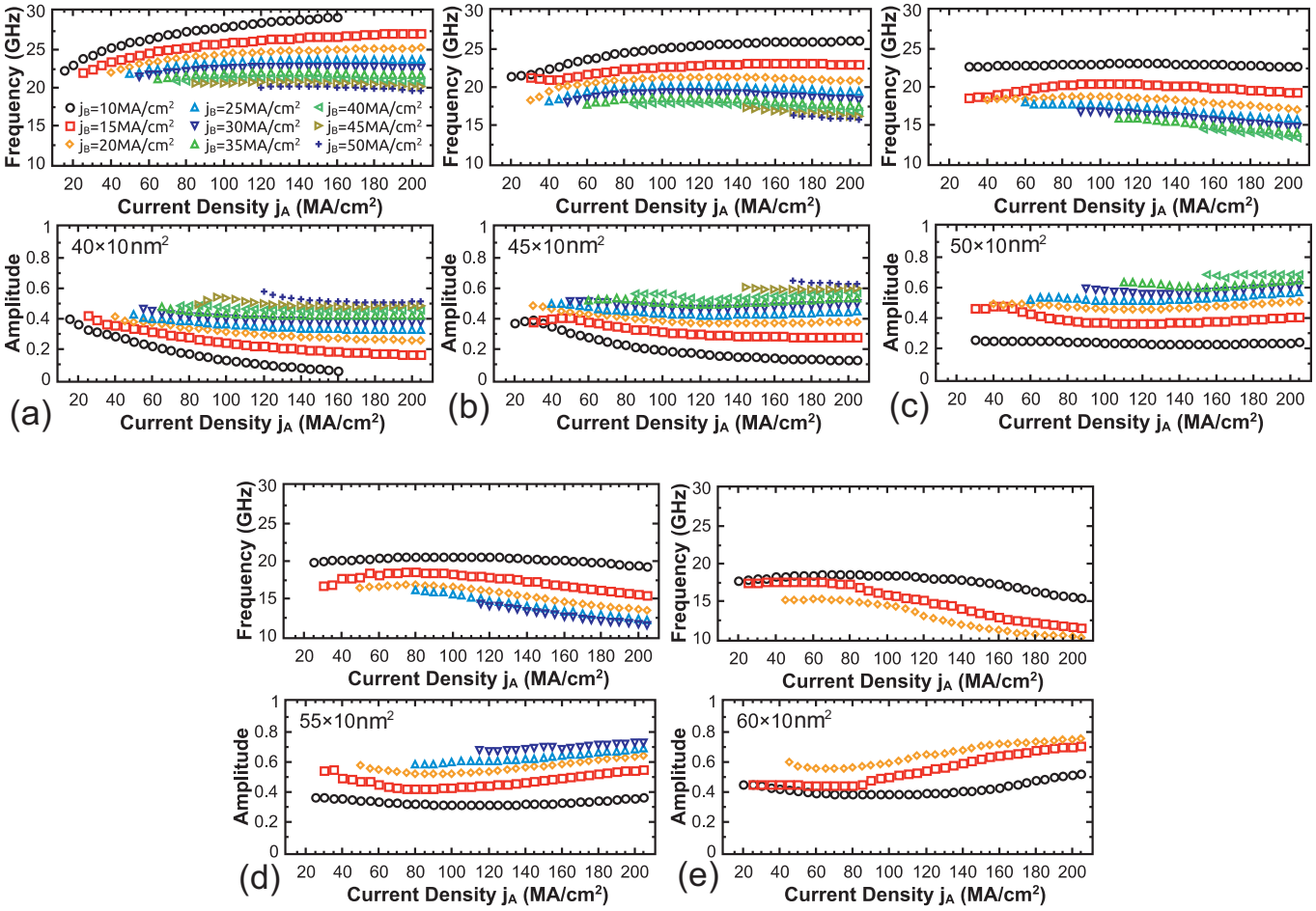

Figure 6. The influence of the device geometry and applied current on oscillation frequency and amplitude $(m_{max}-m_{min})/2$. The dependencies are shown for five lengths of the free layer: 40nm (a), 45nm (b), 50nm (c), 55nm (d), and 60nm (e). The current density through MTJ_A varies from $1\cdot10^7$ to $2.05\cdot10^8$ A/cm^2 using a $5\cdot10^6$ A/cm^2 step size. The current density through MTJ_B for all cases is shown in (a).

REFERENCES

[1] A. Fukushima, T. Seki, K. Yakushiji, H. Kubota, S. Yuasa, and K. Ando, "Statistical variance in switching probability of spin-torque switching in MgO-MTJ", Trans. on Magn., vol. 48, p. 4344, 2012.

[2] Z. Zeng, P. Upadhyaya, P. Khalili Amiri, K. H. Cheung, J. A. Katine, J. Langer, K. L. Wang, and H. W. Jiang, "Enhancement of microwave emission in magnetic tunnel junction oscillators through in-plane field orientation", Appl. Phys. Lett., vol. 99, p. 032503, 2011.

[3] C. H. Sim, M. Moneck, T. Liew, and J.-G. Zhu., "Frequency-tunable perpendicular spin torque oscillator", J. Appl. Phys., vol. 111, p. 07C914, 2012.

[4] Z. Zeng, G. Finocchio, B. Zhang, P. Amiri, J. Katine, I. Krivorotov, Y. Huai, J. Langer, B. Azzerboni, K. Wang, and H. Jiang, "Ultralow-current-density and bias-field-free spin-transfer nano-oscillator" Sci. Rep., vol. 3, p. 1426, 2013.

[5] A. Dussaux, B. Georges, J. Grollier, V. Cros, A. Khvalkovskiy, A. Fukushima, M. Konoto, H. Kubota, K. Yakushiji, S. Yuasa, K. Zvezdin, K. Ando, and A. Fert, "Large microwave generation from current-driven magnetic vortex oscillators in magnetic tunnel junctions", Nature Comm., vol. 1, p. 8, 2010.

[6] A. Makarov, V. Sverdlov, and S. Selberherr, "Magnetic oscillation of the transverse domain wall in a penta-layer MgO-MTJ", Nano.: Phys. and Tech., pp. 338 – 339, 2013.

[7] A. Makarov, V. Sverdlov, and S. Selberherr, "Concept of a bias-field-free spin-torque oscillator based on two MgO-MTJs", SSDM, pp. 796 – 797 , 2013.

[8] A. Makarov, V. Sverdlov, D. Osintsev, and S. Selberherr, "Fast switching in magnetic tunnel junctions with two pinned layers: micromagnetic modeling", Trans. on Magn., vol. 48, p. 1289, 2012.

[9] J. Slonczewski, "Currents, torques, and polarization factors in magnetic tunnel junctions," Phys. Rev. B, vol. 71, p. 024411, 2005.

[10] A. Makarov, V. Sverdlov, and S. Selberherr, "Emerging memory technologies: trends, challenges, and modeling methods," Microelectronics Reliability, vol. 52, pp. 628 – 634, 2012.

[11] M. Iwayama, T. Kai, M. Nakayama, H. Aikawa, Y. Asao, T. Kajiyama et al., "Reduction of switching current distribution in spin transfer magnetic random access memories," J. Appl. Phys., vol. 103, p. 07A720, 2008.